Introduction to Fluidization

Ray Cocco
S. B. Reddy Karri
Ted Knowlton
Particulate Solid Research, Inc. (PSRI)

Fluidized beds offer excellent heat transfer, and have the unique ability to move a wide range of solid particles in a fluid-like fashion. This article explains the basics of fluidization theory and outlines how to design a typical fluidized bed.

Fluidized-bed processes have operated commercially since the 1920s, beginning with the advent of the Winkler coal gasifier in Germany. Fluidized catalytic cracking units (FCCUs) for the production of high-octane gasoline and fluidized-bed reactors for making phthalic anhydride debuted in the 1940s. Today, about three-quarters of all polyolefins are made by a fluidized-bed process.

The development of a specialized zeolite catalyst for cracking heavy oil into various fractions enabled the commercialization of the FCC circulating fluidized bed. In this process, oil is injected into a riser, and the feedstock and catalyst flow upward. As the oil is cracked, a layer of coke (a high-molecular-weight carbonaceous material) builds up on the catalyst, deactivating the catalyst in a matter of seconds. The coke is removed and the catalyst reactivated in a fluidized-bed regenerator.

Fluidized beds typically are more complex to design, build, and operate than other types of reactors, such as packed-bed and stirred-tank reactors. Scaleup of fluidized beds can be difficult *(1)*. Fluidized beds are prone to erosion and particle attrition caused by the moving particles. Solids losses can result in significant operating costs, especially when the solid particles are an expensive catalyst. Bubbles also need to be managed, as large bubbles can travel faster than smaller bubbles in a fluidized bed, which reduces the mass transfer between phases.

Despite these challenges, fluidized beds offer three distinct advantages over other process technologies: superior heat transfer, the ability to easily move solids like a fluid, and the ability to process materials with a wide particle size distribution.

The heat-transfer rate in a fluidized bed can be five to ten times greater than that in a packed-bed reactor. Moving particles, especially small particles, can transport heat much more efficiently than gas alone. Even for the most extreme exothermic reactions, a fluidized bed can maintain an isothermal profile within a few degrees.

The acrylonitrile process, for example, capitalizes on this benefit. The reaction of propylene with ammonia and oxygen has an exothermic heat of reaction on the order of 515 kJ/mol and the product is prone to thermal degradation. Yet, acrylonitrile can be made in a fluidized bed with less than 5°C of variability in the reactor temperature.

Another benefit of fluidized beds is the ability to move solids in a fluid-like fashion. Catalyst can be added or removed from the reactor without requiring a shutdown. Furthermore, in many cases, the entire inventory of catalyst can be removed and replaced in less than a day — whereas it would take many days or weeks to uniformly fill a packed-bed reactor with fresh catalyst. In addition, reactors can be coupled such that the catalyst can be cycled and regenerated; the FCC circulating fluidized-bed reactor is based on this advantage.

Thus, the benefits of using fluidized-bed technology can easily outweigh the disadvantages, especially for processes requiring catalyst circulation or superior heat transfer or both. Reaping these benefits, however, requires a good understanding of fluidization.

Fluidization theory

Particles become fluidized when an upward-flowing gas imposes a high enough drag force to overcome the downward force of gravity. The drag force is the frictional force imposed by the gas on the particle; the particle imposes an equal and opposite drag force on the gas. Thus, as a particle becomes more fluidized, it affects the local gas velocity around it due to these drag forces. This effect is minimal for spherical particles, but the influence of the drag force is more significant for irregularly shaped particles.

Figure 1 shows the increase in pressure drop with increasing superficial gas velocity through a bed of particles that is initially packed. As the superficial gas velocity increases, the pressure drop across the bed increases in accordance with the Ergun equation *(2)*. When the gas velocity is high enough that the drag force on the particles equals the weight of the particles (*i.e.,* $m \times g$), the bed becomes fluidized. This point is commonly referred to as the minimum fluidization velocity, u_{mf}. Higher gas velocities do not create higher pressure drop, because at this point the pressure drop is due solely to the weight of the suspended bed. Thus, the inventory of any fluidized bed can be determined by measuring the pressure drop across the bed and calculating the bed height *(3)*:

$$\Delta P_{bed} = H_{bed} \frac{g}{g_c}\left(\rho_p\left(1-\varepsilon\right)-\rho_g\right) = H_{bed}\frac{g}{g_c}\rho_{bulk} \qquad (1)$$

where ΔP_{bed} is the pressure drop across the bed, H_{bed} is the height of the bed when fluidized, g is the acceleration due to gravity, g_c is the force-weight conversion factor, ρ_p is the particle density, ε is the bed voidage (*i.e.,* gas volume fraction), ρ_g is the gas density, and ρ_{bulk} is the bulk density. The gas density is minimal compared to the bulk density and can be disregarded in Eq. 1.

The minimum fluidization velocity, u_{mf}, can be estimated for spherical particles by first calculating the Archimedes number, Ar:

$$Ar = \frac{\rho_g d_p^3\left(\rho_p-\rho_g\right)g}{\mu^2} \qquad (2)$$

where d_p is the Sauter mean particle size and μ is the fluid viscosity. The Wen and Yu equation *(4)* is a second-order polynomial with respect to the particle Reynolds number calculated at the minimum fluidization velocity, $Re_{p,mf}$:

$$Ar = 1{,}650 Re_{p,mf} + 24.5 Re_{p,mf}^2 \qquad (3)$$

After calculating the Archimedes number, the Reynolds number can be determined using the quadratic equation or an equation solver.

Finally, the minimum fluidization velocity, u_{mf}, can be determined after solving for $Re_{p,mf}$:

$$Re_{p,mf} = \frac{\rho_g u_{mf} d_p}{\mu} \qquad (4)$$

Other minimum fluidization correlations exist, but Eq. 3, based on the work of Wen and Yu *(4),* is the most popular.

When the gas velocities increase beyond the minimum fluidization velocity, bubbles can form. The point at which this occurs depends on the particle size and density. Smaller or lighter particles tend to experience smooth fluidization before bubbles appear. Larger or denser particles tend to start bubbling at the point of minimum fluidization.

The movement of a gas through a fluidized bed can best be described using the two-phase theory *(5)*. According to this theory, gas moves through the bed in two ways — as bubbles, and as part of an emulsion (or dense) phase — as illustrated in Figure 2. The two-phase theory is represented by the equation:

$$Q_{bed} = Q_{emulsion} + Q_{bubbles} = A_{bed}u_{mf} + A_{bed}\left(u_o - u_{mf}\right) \qquad (5)$$

where Q_{bed} is the total gas volumetric flowrate through the bed, $Q_{emulsion}$ is the gas volumetric flowrate through the dense phase, $Q_{bubbles}$ is the gas volumetric flowrate through the bubbles, A_{bed} is the cross-sectional area of the bed, and u_o is the superficial gas velocity.

Up to the minimum fluidization point, all the gas moves through the bed via the emulsion phase. Beyond the minimum fluidization point, any additional gas introduced should travel through the bed as bubbles. Thus, bubbles can be considered as the gas bypassing the process, which is detrimental for mass-transfer-limited processes, such as some heterogeneous reactions. Larger bubbles travel faster than smaller bubbles, so managing bubble size is an important design criterion.

In reality, Eq. 5 is not completely correct. First, small

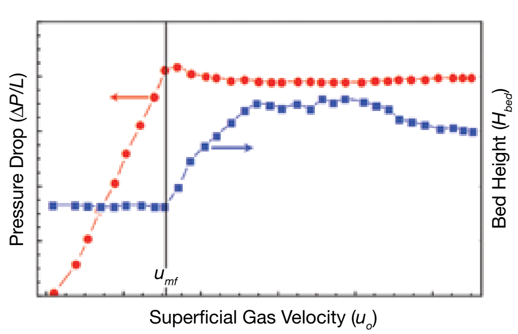

▲ **Figure 1.** This typical minimum fluidization curve shows that the pressure drop (red line) increases with superficial gas velocity until the point at which the gas velocity is high enough that the drag force is equal to the weight of the particle. At this point, the minimum fluidization velocity, the bed becomes fluidized, and the bed height (blue line) increases.

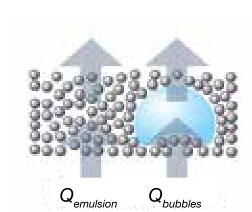

◀ **Figure 2.** According to the theory of two-phase fluidization, gas moves through the particle bed as bubbles and as an emulsion (or dense phase).

particles can experience smooth fluidization before bubbles form (*i.e.,* the region between the minimum fluidization and minimum bubbling velocities). Second, a small amount of gas leaks into and out of the bubbles. Thus, a more accurate version of Eq. 5 is:

$$Q_{bed} = (1-Y)Q_{emulsion} + YQ_{bubbles} = (1-Y)A_{bed}u_{mb} + YA_{bed}(u_o - u_{mb}) \quad (6)$$

where u_{mb} is the minimum bubbling velocity for the onset of bubbles in the bed and Y is the fraction of the gas in the bubbles (which ranges from 0 to 1).

As the gas velocity through the bed continues to increase, the type of fluidization changes, as shown in Figure 3. The bed transitions from a bubbling fluidized bed to a turbulent fluidized bed in which the gas voids are no longer regularly shaped bubbles, but rather have elongated shapes. The top of the bed becomes less well defined due to the increase in entrained particles. At even higher gas velocities, all of the particles are entrained out of the bed. This type of fluidization is called fast fluidization. Further increases in the superficial gas velocity result in complete conveying of all of the particles.

With such variations in bed hydrodynamics based on particle properties, it would seem tedious to predict particle behavior in a fluidized bed. However, Geldart *(6)* provides convenient criteria for predicting the fluidization behavior based on the Sauter mean particle size, d_p, and the particle density. Based on these parameters, particles are classified into four groups: Geldart Groups A, B, C, and D, as depicted in Figure 4. (Note that Figure 4 applies only at ambient temperatures and pressures.)

Geldart Group A. Particles in the Geldart Group A tend to be aeratable and fluidize well. Indeed, most particles used in fluidized beds are Group A powders, mainly because they can be easily made by spray drying.

Group A particle sizes range from 30 µm to 125 µm, and particle densities are on the order of 1,500 kg/m^3. Typically, Group A powders do not promote maximum bubble sizes larger than 20 cm *(7)*. At low gas velocities, Group A powders exhibit significant bed expansion without the formation of bubbles (*i.e.,* smooth fluidization). At high pressure, Group A powders can experience bed expansions of 100% or more. If a fluidized bed is not designed for this type of expansion, it could lose most of its mass to downstream equipment.

The zeolite-based catalysts used in FCC units fall into the Geldart Group A classification. Other fluidized beds, such as catalytic oxidation, oxychlorination, and acrylonitrile processes, also employ catalysts that have a Group A behavior. Most particles used in fluidized beds are Geldart Group A powders.

Geldart Group B. These particles have a particle size range of 150 µm to 1,000 µm. Group B particles tend not to undergo smooth fluidization, and bubbles form at the onset of fluidization. Thus, the minimum fluidization velocity and the minimum bubbling velocity are similar. Group B powders fluidize easily and are used in a wide range of fluidized unit operations with few difficulties. Most fluidized-bed combustors and fluidized-bed pyrolysis units use coal powders with Group B characteristics.

Slugging occurs when the walls of the fluidized bed stabilize the bubbles such that the bubbles push the solids upward in the unit. Group B powders tend to allow the formation of very large bubbles (on the order of meters in tall beds), so slugging can occur in even some large units. Bubble sizes larger than two-thirds the diameter of the bed can cause slugging.

Geldart Group C. Geldart Group C powders are typically less than 30 µm and are the most difficult to fluidize. These particles are considered cohesive, and almost always experience significant channeling (*i.e.,* the formation of a channel of fast moving bubbles that bypass most of the bed) during fluidization. In fact, particles this small tend to

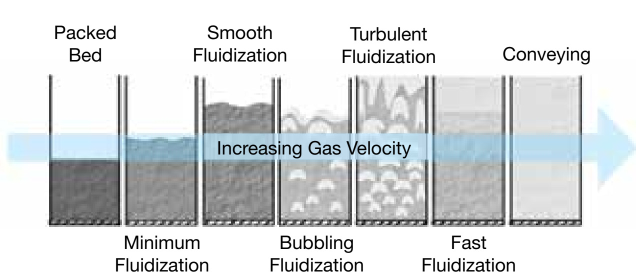

▲ **Figure 3.** As the gas velocity through the bed increases, the type of fluidization shifts.

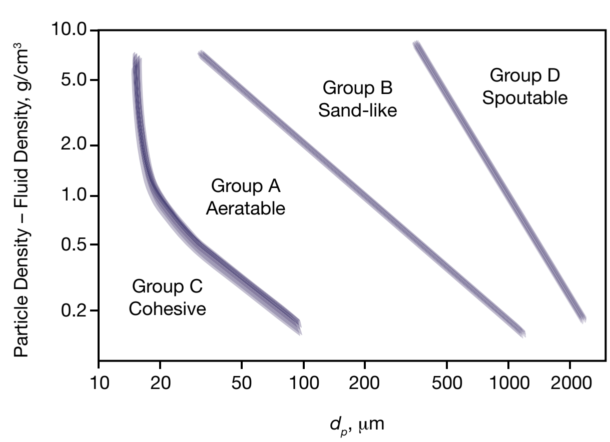

▲ **Figure 4.** The fluidization behavior of particles can be predicted by the Sauter mean particle size and the particle density. Particles are classified into four Geldart groups. Group A particles are typically the easiest to fluidize, while Group C are the most difficult due to their cohesive properties.

behave more as particle clusters than single, independent particles *(8)*. Nanoparticles fall into this classification. To limit this effect, Group C powders are usually fluidized with the aid of baffles, microjets, pulsing, and/or mechanical vibration. Sometimes larger particles, such as Group B powders, are added to the bed to promote smoother fluidization.

Geldart Group D. The largest particles fall into the Geldart Group D classification. The gas requirements for fluidizing Group D powders are large. During fluidization of Group D powders, the bubbles formed are enormous, and slugging can be observed even in large fluidized beds. Thus, these powders are sometimes processed in spouting beds, which have lower gas requirements than standard fluidized beds *(9)*. A spouting bed is a type of fluidized bed in which the gas moves primarily through the center of the bed.

Gas pressure can cause a particle's classification to change, which is not captured in the Geldart chart in Figure 4. Under high pressure, powders of small Group B particles may behave as Group A powders. Furthermore, the transition from one group to another is not well defined. In some cases, the behavior of a powder may fit into more than one classification. For example, some powders fluidize as well as a Group A powder, but become permanently defluidized as a Group C powder once at rest (*i.e.,* consolidation). These powders are sometimes referred to as Group A/C powders.

Fluidized-bed design

A typical fluidized-bed reactor contains a plenum, a gas distributor (such as a grid plate or sparger), the particle bed region, a freeboard region above the particle bed, heating and cooling coils if needed, and cyclones (Figure 5). Some fluidized beds may have a dual feed system consisting of a grid plate with a sparger above it. The acrylonitrile process uses this configuration, in which air is fed through a plenum and distributed by a grid plate while ammonia and propylene are fed through spargers *(10)*. Propylene ammoxidation is highly exothermic (–515 kJ/mol), so heat is removed from the reactor by an array of cooling coils located above the spargers.

Fluidized beds are also used as dryers and heat treaters. Their design is somewhat different from that of a typical reactor. The bed heights in fluidized-bed dryers and heat treaters tend to range from 0.3 m to 0.5 m, whereas fluidized-bed reactors usually have bed heights on the order of 1–10 m.

Several constraints need to be considered in the design of a fluidized bed to ensure reliable operation. The grid plate and sparger are subject to pressure drop and spacing limits. Entrainment rates need to be measured or estimated. Also, cyclones need to be designed for high collection efficiency and low pressure drop.

Distributors

The primary purpose of a grid plate or a sparger is to provide good gas distribution. In addition to pressure drop and spacing considerations, their design also needs to take into account particle attrition, erosion of the vessel and internal components, and mechanical constraints (*i.e.,* thermal expansion, bed slumping during emergency shutdowns, etc.).

Many distributor designs are available (Figure 6). Grid plates can range from simple perforated plates to bubble-

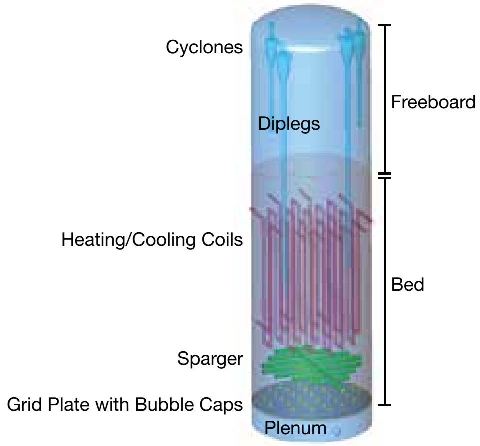

▲ **Figure 5.** A typical fluidized bed has a plenum, a gas distributor, cyclones and diplegs, and heating/cooling coils. This fluidized bed has a dual feed system consisting of both a grid plate and a sparger.

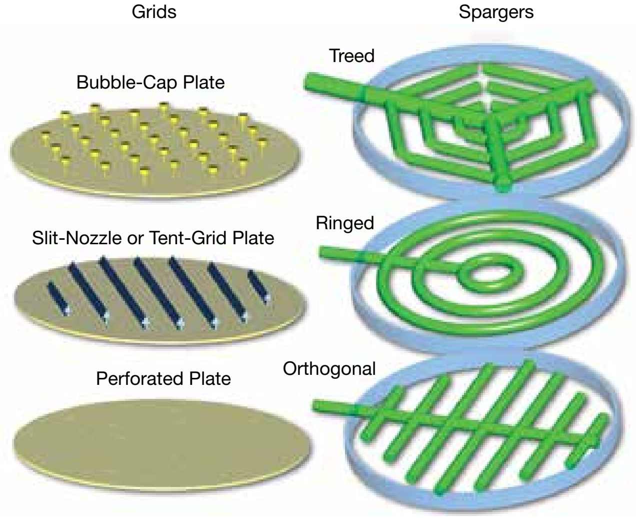

▲ **Figure 6.** Fluidized beds employ a variety of grid plate and sparger designs. Grid plates with bubble caps help reduce particle weeping into the plenum. The most common sparger designs have a treed, ringed, or orthogonal pattern.

cap plates. Bubble cap grid plates are designed to minimize particle weeping into the plenum.

Spargers can be designed with jets that point downward, upward, or laterally. Spargers have the advantage of being easily engineered to accommodate thermal expansion. Common sparger designs have ring, orthogonal, or treed layouts.

Grids and spargers can be equipped with shrouds to minimize particle attrition and to better direct the gas (Figure 7).

Gas (fluid) distribution. The number of orifices and the diameter of the orifices need to be balanced for good gas distribution and pressure drop. If the grid pressure drop is too low, the hydrodynamics of the bed will determine gas flow and the gas will be poorly distributed. This is because the motion of solids and gas in a fluidized bed is comprised of chaotic swirls and eddies, and such motion could create a path of least resistance for the incoming gas or fluid. Thus, it is recommended that a fluidized bed with a relatively tall bed height (greater than 0.3 m) have a pressure drop across each orifice in the distributor or sparger ($\Delta P_{orifice}$) that is at least one-third the pressure drop across the bed *(11)*. Thus, from Eq. 1:

$$\Delta P_{orifice} \geq \frac{1}{3} H_{bed} \frac{g}{g_c} \rho_{bulk} \tag{7}$$

The placement and size of the orifices determine where the gas enters the fluidized bed. If Eq. 7 is not satisfied, then the hydrodynamics of the bed could determine the amount of gas coming from each orifice. In addition, maintaining

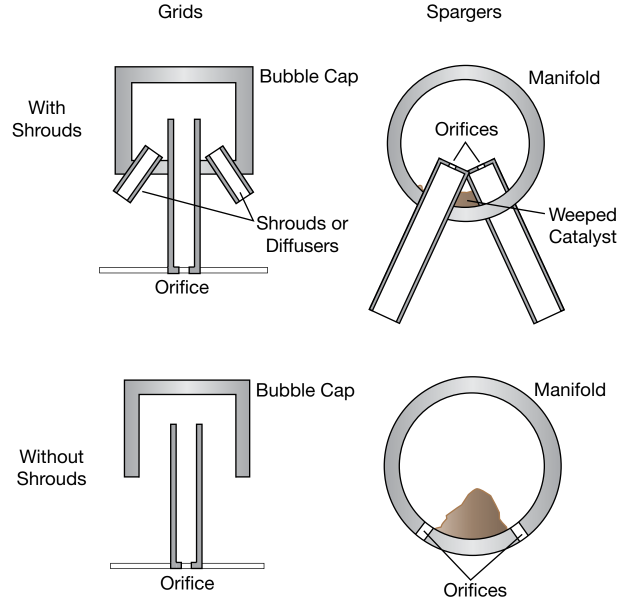

▲ **Figure 7.** The addition of shrouds on bubble caps and spargers can help minimize particle attrition and particle entrainment.

a pressure drop across each orifice above the minimum helps limit particle weeping into the plenum and sparger manifolds.

For shorter fluidized beds such as dryers and heat treaters, the recommended pressure drop across the distributor is the overall bed pressure drop. These units tend to have shallow beds, so Eq. 7 should be expressed as:

$$\Delta P_{orifice} \geq H_{bed} \frac{g}{g_c} \rho_{bulk} \tag{8}$$

Ideally, the pressure drop across a distributor or grid plate should never be less than 2,500 Pa.

Particle attrition and erosion. High particle attrition in a fluidized bed that is not designed correctly can cause losses of tens of millions of dollars per year. To minimize particle attrition:

• use a particle that is designed for such applications

• ensure that high-energy particle collisions in the bed are kept to a minimum.

Particles in a fluidized bed will experience varying levels

Nomenclature

A_{bed}	= cross-sectional area of the bed
Ar	= Archimedes number
d_p	= Sauter mean particle size
$D_{p,50}$	= median particle size within each particle size distribution
g	= acceleration due to gravity
g_c	= force-weight conversion factor
H_{bed}	= height of the bed when fluidized
$m_{collected}$	= total collection rate
m_i	= rate of collection for a particle of diameter *i*
m_{inlet}	= rate of collection at the inlet of the cyclone
ΔP_{bed}	= pressure drop across the bed
$\Delta P_{orifice}$	= pressure drop across each orifice in the distributor or sparger
Q_{bed}	= total gas volumetric flowrate through the bed
$Q_{emulsion}$	= gas volumetric flowrate through the dense phase
$Q_{bubbles}$	= gas volumetric flowrate through the bubbles
$Re_{p,mf}$	= particle Reynolds number calculated at the minimum fluidization velocity
u_{mb}	= minimum bubbling velocity for the onset of bubbles in the bed
u_{mf}	= minimum fluidization velocity
u_o	= superficial gas velocity
x_i	= collection efficiency for a particle of size *i* obtained from the grade efficiency curve
Y	= fraction of the gas in the bubbles (which ranges from 0 to 1)

Greek Letters

ε	= bed voidage (*i.e.,* gas volume fraction)
μ	= fluid viscosity
ρ_{bulk}	= bulk density
ρ_g	= gas density
ρ_p	= particle density

of trauma. The dynamic nature of the bed and the high velocities in the cyclones can cause particles to fragment or abrade. Particle fragmentation is a catastrophic breakup of a parent particle into daughter particles. Abrasion is the removal of small edges and protrusions from the particle surfaces; although the size of the parent particle does not change much, an excess of fines (*i.e.,* particles smaller than 40 μm) may develop.

It should be noted that the crush strength of a particle is not an indication of particle attrition properties. Crush strength testing is relatively static and used mostly for packed-bed applications. Attrition is caused by transient, dynamic forces. Hence, attrition is typically evaluated by ball mill testing *(12)*, jet impact testing, immersed jet testing *(13)*, or jet cup testing *(14)*. The jet cup method, which involves using a tangential gas jet to promote swirling flow in a cylindrical or conical cup *(14)*, is usually used, as it resembles the abrasion caused by a cyclone wall.

Particle attrition occurs when the high-velocity gas jets from the distributor cause particles to collide with each other and with the walls of the vessel. Attrition also occurs when particles carried by the swirling gas flow collide at the cyclone inlet and throughout the cyclone cone region.

It is imperative that gas jets exiting the distributor do not intersect with each other or impact the vessel wall or internals. The velocities of these gas jets can exceed 100 ft/sec (30 m/sec), and particles carried in them can reach velocities of more than 50 ft/sec (15 m/sec). A particle in a gas jet impinging on a wall might experience a 30 mph or higher collision; two particles in impinging jets could collide at more than 60 mph. Furthermore, jets that are too close together can coalesce, which increases particle attrition.

Therefore, the distributor needs to be designed so that the gas jet's penetration length is less than the distance between the orifice and the vessel wall or other internals. This will reduce erosion of the vessel walls and internals as well. The design also needs to ensure that the trajectory of each jet does not intersect with any other jet trajectory.

In order to design a distributor correctly, the appropriate jet penetration length needs to be determined. Published correlations *(15–17)* work well for typical systems with Geldart Group A and B particles. However, there can be a wide variation in results for atypical systems, such as high-pressure fluidized beds and fluidized beds containing nonspherical particles or large particles.

High attrition could still be an issue even if a distributor is designed to minimize jet-wall internal collisions or jet intersections, especially if the particles are fragile. In such cases, shrouds (sometimes called diffusers) can be installed to limit particle entrainment in the jet. Shrouds are sections of piping that extend from each orifice in a grid plate (Figure 7) to shield part of the jet, making it less likely for particles to become entrained. It is important that the shrouds extend far enough to prevent particles from being sucked into the base of the jet.

Structural integrity. Mechanical stress in a fluidized bed can be significant. A power outage can cause the entire bed of material to fall onto the distributor. Thus, the distributor needs to be designed to withstand such forces.

Furthermore, thermal expansion can cause even the thickest distributor to buckle. Thus, the design needs to allow for such expansion. Conical and convex plates have been used successfully for such applications.

In addition, a bubbling fluidized bed has an inherent frequency ranging from 1 Hz to 5 Hz. The harmonics of the distributor plate or sparger need to account for this.

Entrainment

For a particle to be carried out of a bed, the local gas velocity needs to exceed the particle's terminal velocity. Terminal velocity is the speed at which an object in free fall is no longer accelerating. A skydiver's terminal velocity is about 120 mph (155 km/sec). A particle in a bed has a different field of reference. Instead of a body falling through a stagnant fluid, in a fluidized bed, the fluid is moving the body. A particle's terminal velocity is the lowest gas velocity that causes particles to start moving with the gas. This is the point at which entrainment begins.

However, particle entrainment appears to occur well before the superficial gas velocity exceeds the single-particle terminal velocity. While the single-particle terminal velocity is a factor, other factors contribute to entrainment as well. For instance, local gas velocities may be higher than the superficial gas velocity, and small particles may have terminal velocities lower than the local gas velocity. There is often a wide distribution of particle sizes in the bed, and

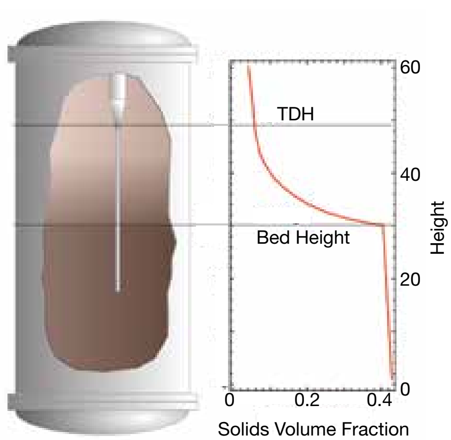

▲ **Figure 8.** The transport disengagement height (TDH) is the point at which larger entrained particles return to the bed, while smaller particles remain entrained.

particle separation based on size (elutriation) may occur. This is common with bubbles that have rise velocities higher than the superficial gas velocity. The momentum of a bubble breaking at the top of a fluidized bed also plays a role in entrainment: As a bubble bursts, particles at the bottom of the bubble can be ejected upward into the freeboard region above the bed *(18)*.

As the gas containing entrained particles flows upward, the larger and/or heavier particles may fall back into the bed. At some distance above the bed, only the smaller particles remain entrained. This point is referred to as the transport disengagement height (TDH). Figure 8 illustrates a typical solids concentration profile for a bubbling fluidized bed and the location of the TDH.

The TDH, entrainment rate, and the size of the particles being entrained are important design parameters for a fluidized bed. The TDH is required because the cyclone or vessel exits are commonly installed at or above the TDH to reduce the solids loading to the cyclones and minimize exit losses. The entrained particle size distribution is needed to size the cyclones and determine the resulting collection efficiency. The entrained particle size distribution is also used, with the entrainment rate, to estimate the solids loss rate, which is required to specify the size of the cyclone dipleg. Diplegs designed based on an entrainment rate that is too high or too low are prone to plugging.

Empirical entrainment rate correlations are available *(19–24)*, but their accuracy is tied to the systems from which the data were collected. As a result, entrainment rate correlations can vary by two orders of magnitude, especially for particles smaller than 50 μm. The variability among entrainment rate correlations occurs, in part, because the correlations were derived based on the assumption that particles in a fluidized bed behave independently of each other. This may not be the case for small particles, which can form weakly bound clusters that have a larger aerodynamic diameter and are less likely to be entrained than the lone particles *(8)*. Therefore, it is recommended that when designing a system with a new or untested type of particle, the entrainment rate should first be measured experimentally before using a correlation that has not been validated or completing computational fluid dynamics modeling.

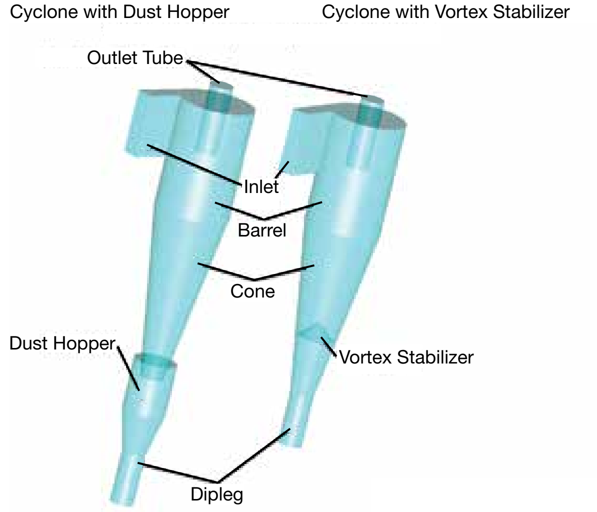

▲ **Figure 9.** In a reverse-flow cyclone separator, entrained particles enter from the top of the cyclone. Centrifugal forces separate the solids from the gases. The particles spiral down the barrel and cone region and exit via the dipleg. The gas exits through the outlet tube.

Cyclones

The gases from a fluidized bed usually need to be cleaned of entrained particles. In commercial-sized units, particle entrainment can be significant, and the particles often need to be collected and returned to the bed. Cyclone separators (Figure 9) are typically employed for such applications.

RAY COCCO is the President and CEO of Particulate Solid Research, Inc. (PSRI), a consortium-based company with 32 member companies in Canada, France, Brazil, Finland, Germany, India, South Africa, Saudi Arabia, and the U.S. Before joining PSRI, he was with the Dow Chemical Co. for 17 years as a technical research leader. He was Chair of the AIChE Particle Technology Forum (Group 3), is a board member of ASTM's D18.24 Committee on Characterization and Handling of Powders and Bulk Solids, and is on the Editorial Advisory Board for *Powder and Bulk Engineering* and *Powder Technology.* He is a member of AIChE's Chemical Engineering Technology Operating Council (CTOC), and the Advisory Boards for the Univ. of Florida's Chemical Engineering Dept., Auburn Univ.'s Chemical Engineering Dept., and Centre of Nature Inspired Engineering at Univ. College London. Cocco is also a member of the International Fluidization Conference Advisory Committee and the meeting chair for the next World Congress in Particle Technology (WCPT8). He has 40 publications, three book chapters, three patents and patent applications, and numerous invited presentations. He consults for industry, national labs, and universities on a regular basis. Cocco received his BS in chemical engineering from the Univ. of Florida and his PhD from Auburn Univ.

S. B. REDDY KARRI is an engineering director at PSRI. He is an expert in the area of fluid-particle systems, such as fluid beds, cyclones, diplegs, standpipes, and risers. He extensively consults and troubleshoots industrial problems in the energy field. He is currently Chair of the Fluidization and Fluid Particle Systems Subcommittee of the Particle Technology Forum. He has written over 100 papers in the area of fluid-particle systems, and has been teaching PSRI technical seminars to industrial engineers from all over the world for the last 20 years. Karri received his BS in chemical engineering from the Univ. of New Hampshire.

TED KNOWLTON is a research fellow at PSRI. Previously, he was the head of the Fluidization Research and Consulting Group of the Institute of Gas Technology (IGT). He is recognized worldwide as an authority in the field of fluidization, fluid-solid contacting, and solids transport. He developed the L-valve, a nonmechanical device that controls solids flow in high-pressure, high-temperature systems. He received the Distinguished Service Award from the Fluidization and Fluid-Particle Systems Committee of AIChE in 1990, the Fluor Daniel Lectureship Award for his contributions to the area of fluidization in 1996, and the Thiele Award for outstanding lifelong contributions to the field of chemical engineering in 2004. He has authored over 120 technical articles and three book chapters, has edited several books on fluidization, and holds four patents. Knowlton received his BS and PhD in chemical engineering from Iowa State Univ.

Article continues on next page

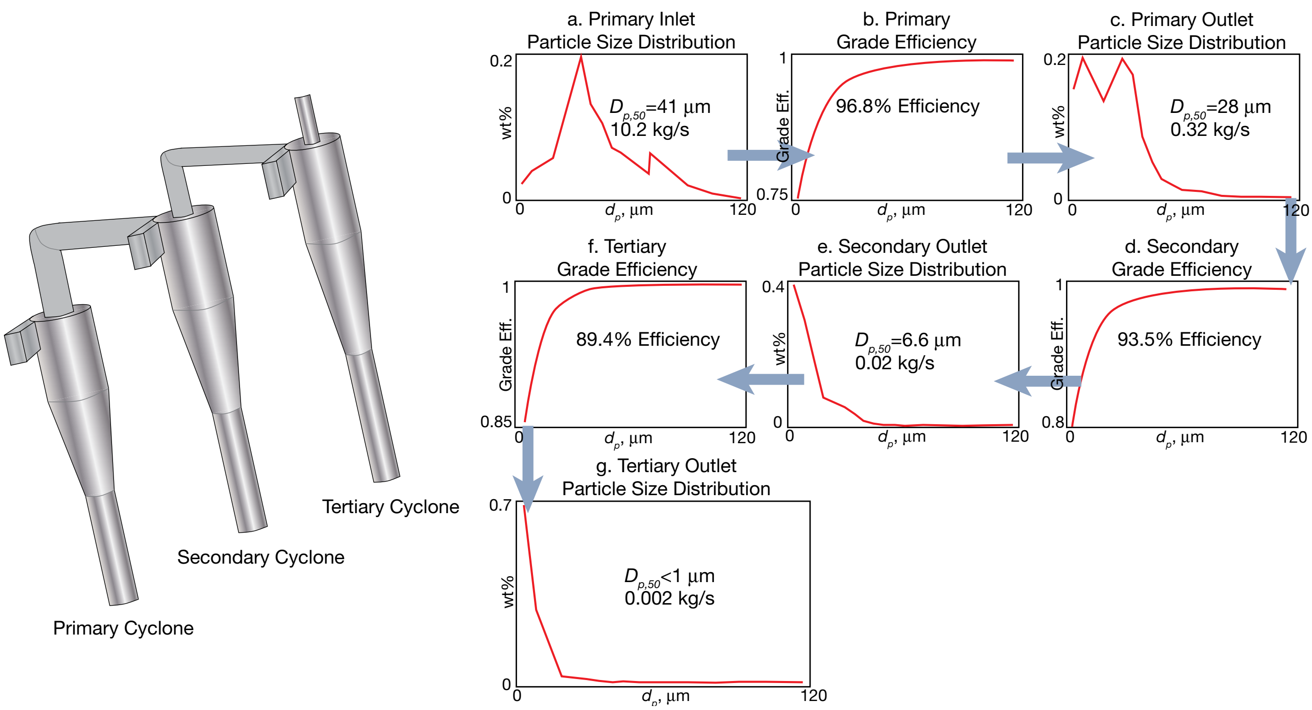

▲ **Figure 10.** Solids losses can be reduced by using a train of cyclones. In this example, adding secondary and tertiary cyclones after the primary cyclone reduces the solids losses from 10.2 kg/sec to 0.002 kg/sec. The $D_{p,50}$ is the median particle size within each particle size distribution (PSD).

The most common type of cyclone separator used in fluidized beds is the reverse-flow cyclone (Figure 9), which consists of an inlet connected tangentially to a barrel section with a conical exit at the bottom. An outlet tube (or vortex finder) extends from the top of the barrel section. Momentum pushes the incoming particles toward the wall, where centrifugal forces cause gas-solid separation. The particles, which experience forces as high as hundreds of times the force of gravity, spiral down the barrel and cone region and exit through the dipleg. Most of the gas reverses its flow, typically in the cone region, and exits through the outlet tube. This reverse flow of gas has a tighter spiral, which provides a second stage of separation with even higher forces that move the particles back to the wall. Thus, the name — reverse flow cyclones.

The collection efficiency of a cyclone can be estimated from a grade efficiency curve — a plot of the probability that a particle of a particular size can be collected. Smaller particles are less likely to be collected than larger particles unless they cluster or agglomerate. Correlations are available *(25, 26)* to construct the cyclone grade efficiency curve based on design parameters, operating conditions, and physical properties.

For most fluidized-bed applications, one cyclone is not enough. Suppose the entrainment rate from the exit of a fluidized bed is measured at 10 kg/sec and the particle size distribution has a median size, or a $D_{p,50}$, of 41 µm (Figure 10a). This corresponds to a solids loss rate of more than 850 m.t./day. Even for a low-cost solid, such a loss rate translates to hundreds of millions of dollars a year. Furthermore, the downstream equipment would need to be cleaned to remove particle buildup, adding another cost. The addition of cyclone separators can reduce these losses 100-fold or more.

The grade efficiency curve for the primary cyclone (Figure 10b) allows the particle collection efficiency to be determined from:

$$m_i = m_{inlet} x_i \tag{9}$$

$$m_{collected} = \sum_{i=1}^{n} m_{inlet} x_i \tag{10}$$

where m_i is the rate of collection for a particle of diameter i, m_{inlet} is the rate of collection at the inlet of the cyclone, x_i is the collection efficiency for a particle of size i obtained from the grade efficiency curve, and $m_{collected}$ is the total collection rate. The primary cyclone reduces the loss rate to 0.32 kg/sec, and the particle size distribution shifts and now has a median of 28 µm (Figure 10c). This corresponds to an overall cyclone collection efficiency of 96.8%.

Even with a 96.8% collection efficiency for the primary cyclone, losses will amount to millions of dollars per year.

A secondary cyclone installed downstream of the primary cyclone's outlet tube reduces the loss rate to 0.02 kg/sec (Figure 10e). If that rate is still too high, a tertiary cyclone can be added to reduce the loss rate further, to 0.002 kg/sec (Figure 10g). A train of cyclones such as this can reduce the costs due to particle losses from the fluidized bed from tens of millions of dollars per year to hundreds of thousands of dollars.

Adding more cyclones beyond three is usually not cost-effective. As the median size of the particles exiting successive cyclones decreases, the probability of collection by a subsequent cyclone decreases (Figures 10b, 10d, and 10f) and the collection efficiency decreases.

Cyclones are often located within the fluidized bed, as this reduces capital costs, especially for beds operating at high pressures. Some pilot units, dryers, and heat treaters have external cyclones. A disadvantage of internal cyclones is that they are difficult to access for servicing. Because cyclones are a common source of reliability problems, servicing capabilities need to be considered.

Closing thoughts

Many new fluidizing processes are emerging, including biomass gasification and pyrolysis, coal gasification, polycrystalline silicone synthesis (for solar panel manufacturing), chemical looping (for carbon dioxide sequestration), methane coupling, gas-to-liquid (GTL) conversion, and propane dehydrogenation, to name a few. Fluidized beds can be an effective unit operation if designed correctly. In addition to the factors discussed here, other important considerations include the management of fines, bed expansion, pressure effects, and potential gas bypassing. With proper engineering, fluidized beds can provide years of reliable, economical service. CEP

Literature Cited

1. **Merrow, E.,** "Linking R&D to Problems Experienced in Solids Processing," Rand Report No. P-7034, Rand Corp., Santa Monica, CA, pp. 1–23 (Nov. 1984).
2. **Ergun, S.,** "Fluid Flow through Packed Columns," *Chem. Eng. Progress,* **48,** pp. 89–94 (1952).
3. **ASTM International,** "Standard Test Method for Measuring the Minimum Fluidization Velocity of Free Flow Powders," ASTM D7743-12, ASTM, West Conshohocken, PA (2012).
4. **Wen, C. Y., and Y. H. Yu,** "A Generalized Method for Predicting the Minimum Fluidization Velocity," *AIChE Journal,* **12,** pp. 610–612 (1966).
5. **Toomey, R. D., and H. F. Johnstone,** "Gaseous Fluidization of Solid Particles," *Chem. Eng. Progress,* **48** (5), pp. 220–226 (May 1952).
6. **Geldart, D.,** "Types of Gas Fluidization," *Powder Technology,* **7,** pp. 285–292 (1972).
7. **Kunni, D., and O. Levenspiel,** "Fluidization Engineering," 2nd ed., Butterworth-Heinemann, Boston, MA (1991).
8. **Cocco, R. F., *et al.*,** "Particle Clusters in and above Fluidized Beds," *Powder Technology,* **203,** pp. 3–11 (2010).
9. **Epstein, N., and J. R. Grace,** "Spouting of Particulate Solids" in "Handbook of Powder Science and Technology," Fayed, M. E., and L. Otten, eds., Springer, NY, pp. 532–567 (1997).
10. **Grasselli, R. K.,** "Handbook of Heterogeneous Catalysis: Vol. 1," Ertl, G., *et al*., eds., 2nd ed., Wiley-VCH, p. 2302 (1997).
11. **Karri, S. B. R., and T. Knowlton,** "Gas Distributor and Plenum Design in Fluidized Beds," in "Fluidization Solids Handling and Processing," Yang, W.-C., ed., Noyes Publications, Westwood, NJ, pp. 209–235 (1999).
12. **ASTM International,** "Standard Test Method for Attrition and Abrasion of Catalysts and Catalyst Carriers," ASTM D4058-96, ASTM, West Conshohocken, PA (Mar. 2006).
13. **ASTM International,** "Standard Test Method for Determination of Attrition and Abrasion of Powdered Catalysts by Air Jets," ASTM D5757-00, ASTM, West Conshohocken, PA (Dec. 2004).
14. **Cocco, R., *et al.*,** "Jet Cup Attrition Testing," *Powder Technology,* **200,** pp. 224–233 (2010).
15. **Shakhova, N. A.,** "Discharge of Turbulent Jets into a Bed," *Inzhenerno-Fizicheskii Zhurnal,* **14** (1), pp. 61–69 (1968).
16. **Zenz, F.,** "Bubble Formation and Grid Design," *Institute of Chemical Engineering Symposium Series,* Ser. 30, p. 136 (1968).
17. **Merry, J. M. D.,** "Penetration of Vertical Jets into Fluidized Beds," *AIChE Journal,* **21** (3), pp. 507–510 (1975).
18. **Davidson, J. F., and D. Harrison,** "Fluidized Particles," Cambridge University Press, Cambridge, U.K. (1963).
19. **Zenz, F., and N. A. Weil,** "A Theoretical-Empirical Approach to the Mechanism of Particle Entrainment from Fluidized Beds," *AIChE Journal,* **4** (4), pp. 472–479 (1958).
20. **Geldart, D., *et al.*,** "The Effect of Fines on Entrainment from Gas Fluidized Beds," *Transactions of the Institute of Chemical Engineering,* **57,** pp. 269–277 (1979).
21. **Lin, L., *et al.*,** "Elutriation and Attrition of Char from a Large Fluidized Bed," *Powder Technology,* **27** (1), pp. 105–115 (1980).
22. **Colakyan, M., *et al.*,** "Elutriation from a Large Particle Fluidized Bed with and without Immersed Heat Transfer Tubes," *Chem. Eng. Progress Symposium Series,* **77** (205), pp. 66–75 (1981).
23. **Colakyan, M., and O. Levenspiel,** "Elutriation from Fluidized Beds," *Powder Technology,* **38,** pp. 223–232 (1984).
24. **Stojkovski, V., and Z. Kostic,** "Empirical Correlation for Prediction of the Elutriation Rate Constant," *Thermal Science,* **7,** pp. 43–58 (2003).
25. **Leith, D., and W. Licht,** "The Collection Efficiency of Cyclone Type Particle Collectors — A New Theoretical Approach," *Chem. Eng. Progress Symposium Series,* **68** (126), pp. 196–206 (1972).
26. **Hoffmann, A. C., and L. E. Stein,** "Gas Cyclones and Swirl Tubes: Principles, Design and Operations," 2nd ed., Springer, Heidelberg, Germany (2008).